

# Electronic Nose Detection of Hydraulic-Oil Fingerprint Contamination in Relevant Aircraft Maintenance Scenarios

M. Salvato, S. De Vito, M. Miglietta, E. Massera, E. Esposito,  
F. Formisano, G. Di Francia and G. Fattoruso

**Abstract** Modern aircraft structure, by making use of lightweight composite materials based on carbon fiber reinforced plastics (CFRP), succeeds in reducing CO<sub>2</sub> emissions and transport fuel costs. Nevertheless, its usage cannot leave Non Destructive Tests out to consideration in order to set up a quality assurance procedure of surfaces' contamination status. Here, we show and compare two different e-nose solutions able to detect and quantify hydraulic-oil fingerprint contamination at significantly low contamination levels occurring during aircraft maintenance operations.

**Keywords** Electronic nose · Aerospace industrial application  
Maintenance scenarios · Non destructive test

## 1 Introduction

In the aerospace industry, the carbon fiber reinforced plastics (CFRP) usage, making weight-light the aircraft primary structures, guarantees a considerable improvement on engine efficiency leading to an important saving in terms of fuel costs (up to 20%), cost efficiency for ground operations (up to 50%) and CO<sub>2</sub> emissions (up to 15% on a per-mile-passenger basis) [1, 2]. Nevertheless, the lack of adequate quality assurance protocol based on Non Destructive Tests (NDT) could be prevent their usage. Indeed, CFRP panels are assembled through adhesive bonding instead of classical riveting. The bond strength is straightly linked with the cleaning state of the composite joints because of its influence on their mechanical properties weakening. Indeed, panel contamination status may produce

---

M. Salvato (✉) · S. De Vito · M. Miglietta · E. Massera · E. Esposito · F. Formisano ·  
G. Di Francia · G. Fattoruso  
DTE-FSN-DIN lab, ENEA—Italian National Agency for New Technologies Energy  
and Sustainable Economic Development, C.R. Portici, P.Le E. Fermi, 1,  
80055 Portici (NA), Italy  
e-mail: Maria.Salvato@enea.it

a reduction in mode-I and -II fracture toughness, leading to interlaminar tension ( $G_{IC}$ ) and sliding shear ( $G_{IIC}$ ) [3], jeopardizing bonding reliability. So, an efficient NDT procedure has to be able to detect and eventually estimate the CFRP panel contamination level occurring during assembly and maintenance operations. In this work, we mainly focus on the contamination affected by Fingerprint/Skydrol, a fire-resistant aviation hydraulic oil used during ordinary operative life operations on the aircraft structures. An efficient NDT assessment protocol e-nose based, enhanced by an ad hoc PARC system architecture, is already carried out during the just ended FP7-ENCOMB project [4, 5]. The ENCOMB experimental setting, characterized by laboratory environment and high panels contamination levels, allowed to put Technology Readiness Level (TRL) of that NDT procedure in the low-end (1–3) of its scale. In order to uplift and extend the TRL of such methodology, in the new European project (H2020-COMBONDT), the application scenarios have been adapted to be more similar to real aircraft maintenance conditions. Substantially, contamination concentration levels have been chosen so that they are significantly lower than previous ENCOMB ones. So, tools and methodologies are conveniently re-adapted at this aim. In this work, we propose two e-nose solutions, one commercial and other one made in ENEA, together with two different sampling methods. Data gathered from each of these different experimental settings are examined by means of principal component analysis allowing to select the setup (e-nose and sampling method) more sensitive to CFRP panel Fingerprint/Skydrol contamination. Analysis performed has shown that the sampling method based on a pre-chemical surface treatment, enhancing e-nose uptake capabilities, helps to mitigate some inherent e-nose limitations in Fingerprint/Skydrol detection. Indeed, both devices, taking advantage from this new sampling method, seem able to improve their hydraulic-oil fingerprint detection capabilities at least at the highest contamination level as well as regression capabilities in the estimation of contamination level. This work is so organized: Section 2 mainly concerns the description of experimental setting (maintenance contamination, e-nose technologies); the problem statement is introduced in the Sect. 3; Sect. 4 is devoted to classification and regression results.

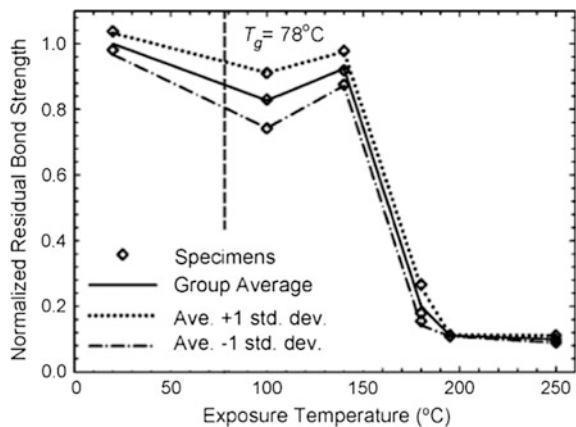
## 2 Experimental Framework

In this section, contamination conditions occurring in aircraft maintenance scenario together with needed tools to detect CFRP panel affected status are described. Generally, the repair operations, to be performed on aircraft structure to ensure airworthiness during the flight, are almost four and vary in scope, duration and frequency [6]. Here, we refer to heavy scheduled maintenance operations during which repairing actions have been carried first, removing outer damaged layers and locally scarfing them, and then substituting them with patches bonded on. In the pre-bond phase, NDT tests are needed to check the cleaning state of the involved surfaces and assuring a reliable and maximum bond strength.

## 2.1 Maintenance Contamination Setup

During the scheduled aircraft maintenance operations, several types of contaminations could be occurred on the CFRP panel surfaces compromising their cleaning state and so potential bonds' strength. In order to perform our NDT technology, testing samples have to reproduce almost exactly the potential contaminations occurring on the CFRP panels during real maintenance operations. Involved Panels' surface are composed by a Carbon Fiber Reinforced material, i.e. a thermoset matrix with carbon fibres arranged in unidirectional layers (HexPly<sup>®</sup> M21 matrix from Hexcel and T700 low density carbon fibers). The degradation process is conducted in a such way as to yield different contamination level, each of one causing a loss of bond strength of 30% of the previous one, starting to a no defective panel status (marked with RE). The reference status of a panel has been degraded by means of chemical or physical treatment. In the first case, panel surface has been compromised by a de-icer fluid or an aviation hydraulic-oil. In the latter case, surface damage has been caused by panel exposure to high temperatures so to generate thermal degradation of its structure. In both cases, three different damage levels have been considered by a project partner with specific expertise in this application field. The hydraulic oil contamination is artificially applied to the surfaces using a gloved plastic finger simulator previously dipped in a mixture composed by different concentrations of Skydrol<sup>®</sup> 500-B, an aviation hydraulic fluid, and heptane. The three different contamination levels correspond respectively at 20, 50, 100% (no dilution) of Skydrol in heptane. Potassium formiate based runway de-icer fluid has been characterized by XRF as producing increasing percentage of potassium at surface in the ranges ([6.4 ( $\pm 1.8$ ); 10.9 ( $\pm 2.3$ ); 12.0 ( $\pm 1.4$ )] at% K). Thermal degradation procedure provides for a heat treatment of panels, at three different temperatures (220 °C; 260 °C; 280 °C), for 2 h. Indeed, starting from 150 °C, as illustrated in Fig. 1, the bond strength decayed significantly.

**Fig. 1** After high-temperature exposure, the residual bond strength properties of FRP systems decay significantly starting from 150 °C [7]





sensors and unheated chemiresistors based on nanostructured semiconductors. Modularity of its hardware is designed to involve innovative technologies and/or new requirements.

The setting adopted in this context includes 6 metal-oxide (MOX) and 1 photo-ionization detector (PID), temperature and relative humidity sensors. Moreover, multi-sensor array contains also 6 custom conductometric graphene based. The measurement process begins with a baseline phase during which sensors have to stabilize their resistance in a reference environment composed by filtered air. In the following acquisition phase, data are fetched measuring the variation of sensor resistance when SNIFFI is exposed to the volatiles coming off the contaminated panel surface (Fig. 4).

In order to catch dynamic characteristics in the sensor array response, several features, differently typified for each device, are extracted. In Table 1, the description of the 40 features, computed on 8 GDA-2 signal sensors is reported.

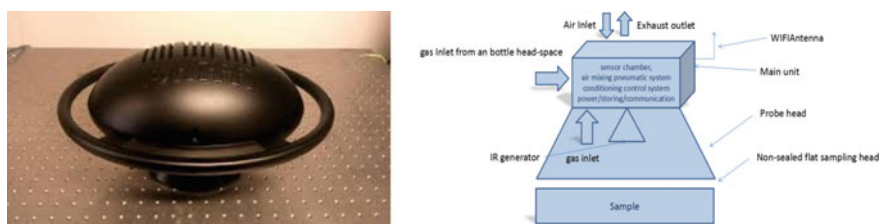
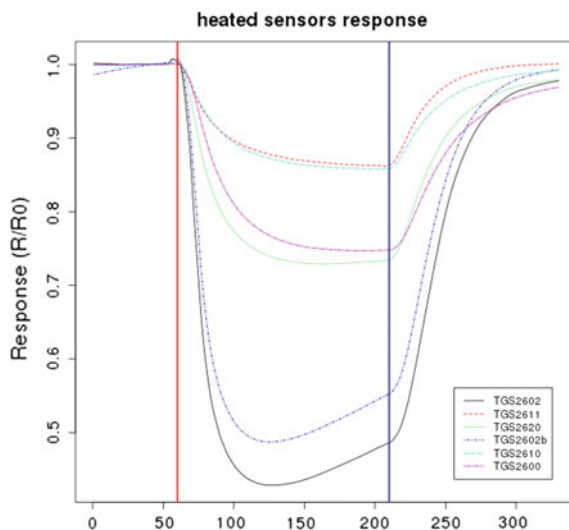


Fig. 3 Sniffi design (on the left) and block design of SNIFFI working system (on the right)

Fig. 4 MOX sensors response to Fingerprint/Skydrol at the highest available concentration



**Table 1** Description of the GDA-2 features from 8 sensors

# Feature	Description
Feature 1 ( $\times 8$ )	Uptake phase derivative
Feature 2 ( $\times 8$ )	Steady state response derivative
Feature 3 ( $\times 8$ )	Desorption phase derivative
Feature 4 ( $\times 8$ )	Uptake phase average
Feature 5 ( $\times 8$ )	Steady state response average

**Table 2** Description of the SNIFFI features extracted from MOX and PID sensors

# Feature	Description
Feature 1 ( $\times 7$ )	Steady state response (wrt avg baseline)
Feature 2 ( $\times 7$ )	Steady state response—IROff (wrt avg baseline)
Feature 3 ( $\times 7$ )	Desorption status (wrt avg baseline)
Feature 4 ( $\times 7$ )	Uptake derivative
Feature 5 ( $\times 7$ )	Desorption derivative
Feature 6	Temperature
Feature 7	Relative humidity

In Table 2, SNIFFI features, extracted taking in account of 6 MOX, 1 PID and temperature and relative humidity sensors, are described.

### 3 Problem Statement

Our main issue concerns the detection on the CFRP panel of Fingerprint/Skydrol contamination and eventually the estimation of its concentration. So, we have in mind to address a 2-class pattern recognition problem into two different stages. Firstly, we aim to distinguish the Fingerprint/Skydrol contaminated class, independently from the concentration level, from the class of interferences. By interferences, we mean all other contaminants, including reference samples, differing from Fingerprint/Skydrol contaminated samples. At the second level, we try to estimate the Fingerprint/Skydrol concentration level.

First of all, in this section we deal with the issue concerning the sampling method to be adopted. At this aim, separation capabilities of two different sampling methods are assessed taking advantage of principal component analysis on data fetched from each e-nose.

#### 3.1 Sampling Methods

In the framework of e-nose sampling method, generally the standard “0-method” has been considered. It basically makes use of no additional treatment on the

**Table 3** Total amount of data sampled by 0-Method

Data sampled by 0-Method		
	GDA-fr	SNIFFI
FP-1	0	0
FP-2	2	1
FP-3	6	6
ALL	17	18

FP refers to Skydrol contaminated samples at low (1), medium (2) and high (3) concentration level. ALL includes not Skydrol contaminated samples: untreated (Reference) plus interferences (TD, DI) samples

sample. Easily, the CFRP sample is positioned close to the e-nose gas inlet, not more than 4 mm distance, while the extraction of volatiles compounds from the sample surface is aided by switching on the IR emitter. The lighting time is different depending on the employed e-noses. In the Table 3, we report the total amount of measurements sampled by this method. FP tag indicates the Skydrol fingerprint contamination; while -1, -2, -3 are respectively low, medium and high contamination level. Instead, ALL is the mark gathering all other interferences, such as thermal degradation, de-icer fluid contamination and reference samples.

In order to point out the robustness of this sampling method, Principal Component Analysis (PCA) has been performed on the acquired normalized data. This analysis helps in exploring data capabilities to disclose the surface contamination if it occurs. Indeed, according to this technique, multi-dimensional data are projected in a new orthogonal space whose dimensions, linearly correlated with initial ones, are ranked according to the increased amount of data signal variance. Formally, let be data matrix  $X$  and its variance-covariance matrix

$$X = \begin{pmatrix} X_1 \\ \vdots \\ X_p \end{pmatrix}, \quad \text{Var}(X) = \Sigma = \begin{pmatrix} \sigma_1^2 & \cdots & \sigma_{1p} \\ \vdots & \ddots & \vdots \\ \sigma_{p1} & \cdots & \sigma_p^2 \end{pmatrix}$$

and the following linear combinations:

$$\begin{aligned} Y_1 &= e_{11}X_1 + \dots + e_{1p}X_p \\ &\vdots \\ Y_p &= e_{p1}X_1 + \dots + e_{pp}X_p \end{aligned}$$

where  $e_{11}, \dots, e_{ip}$  can be viewed as regression coefficients. The *first principal component* is the linear combination of  $X_i$ -variables that explain maximum variance, specifically we will select  $e_{11}, \dots, e_{1p}$  that maximizes  $\text{Var}(Y_1)$  subject to the constraint that  $\sum_{j=1}^p e_{1j}^2 = 1$ , required so that a unique solution may be obtained. In general, for  $i$ -th principal component,  $e_{i1}, \dots, e_{ip}$  are selected in a way to maximize

$$Var(Y_i) = \sum_{k=1}^p \sum_{l=1}^p e_{ik}e_{il}\sigma_{kl}$$

with the following constraints:

$$\sum_{j=1}^p e_{ij}^2 = 1 \quad \text{and} \quad cov(Y_1, Y_i) = cov(Y_2, Y_i) = \dots = cov(Y_{i-1}, Y_i) = 0$$

The coordinates of the original data in the new orthogonal space are named “scores”. Score plot allows to have easier data visualization than the original dataset. So, in the following figures, each 1-sigma ellipse has been built clustering scores related to each fixed contaminant at a given contamination level. By choosing two, among the first three principal components, the centers are computed as means of scores along these components, while major and minor semi-axes correspond to standard deviations (1-sigma) of these ones. Particularly, the 2-dimensional ellipses have drawn by means of following equations:

$$X = mean(A) + std(A) * \cos t$$

$$Y = mean(B) + std(B) * \sin t$$

being A and B, respectively, data scores along two of principal components, while “std” is the standard deviation and  $t$  is the parameter in  $[0, 2\pi]$ . Specifically, ALL-ellipse groups scores related to all contaminants i.e. (TD, DI and reference sample) differing from Skydrol/FingerPrint (FP) contaminated samples. So, ALL-ellipse is the cluster of interferences, while FP-ellipses gather the Skydrol/FingerPrint contaminations according to the different contamination level. As regards data sampled by 0-method, Fig. 5 clearly depicts the different e-noses

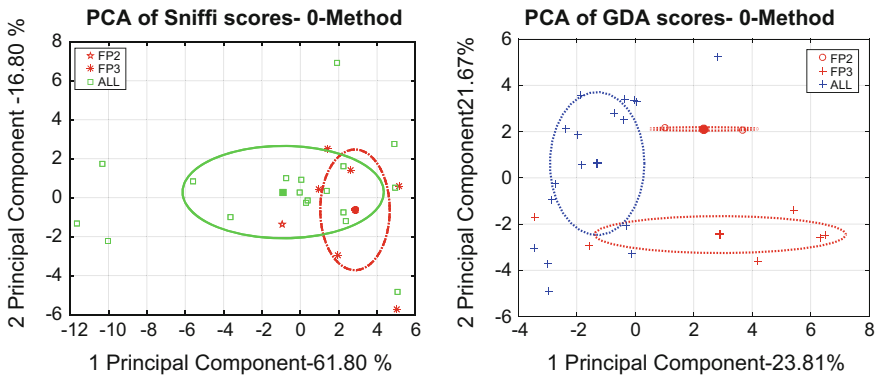


**Fig. 5** PCA of scores related to Sniffi and GDA-2 response sampled by 0-method. FP cluster at each contamination levels (2–3) and all other interferences (ALL) cluster are highlighted



response. At the left, we can see as SNIFFI response does not allow for a sufficient 1-sigma level of separation between Skydrol contaminations and interferences cluster. The wide variance oscillation range in the interferent distribution makes it weakly distinguishable from FP distribution. Otherwise, GDA-fr response highlights good capability to discriminate both FP from all other contaminants as well as Skydrol contamination level.

Because of underlined weak SNIFFI capabilities to discriminate FP contamination when it is sampled by means of 0-method, further adaptations in the sampling system has been allowed to emphasize the contamination sensitivity of both devices. The new method foresees the use of a low-boiling solvent over the sample surface allowing to improve the desorption of the volatiles and differentiate the surfaces according to the capacities to retain and desorb the solvent. The wetting process is performed spraying few millilitres of ethanol with an airbrush over the surface of the sample. Because of chemical treatment, this sampling method is indicated as “PC-method” (where PC stands for “Probe Chemical”). The treatment time spanned on each CFRP sample must not last for more than 2 min. Contamination sampling sequence has been randomly executed but at every hour a test performed on a reference sample ensures that boundary conditions (process poisoning and/or environmental setting) are not changed. In the Table 4, the total amount of measurements executed by PC-method.

In Fig. 6, PCA analysis, performed on CFRP panels sampled by PC-method, underlines an overall improvement in the Skydrol/Fingerprint discrimination capability for both devices. In particular, SNIFFI response seems more sensitive at least to the highest concentration level Skydrol/Fingerprint contamination. Indeed, a consistent, more than 1-sigma, separation distance appears between FP-3 and the other contamination levels, like FP-2 and FP-1. These latter samples are however even hardly distinguishable among all other interferences. On the other hand, the already GDA e-nose good enough discrimination capabilities are enhanced by PC-method sampling. Each FP contaminated level is clearly distinguishable from each other by a consistent more 1-sigma level of separability.

So, PC-method shows an overall improvement of both e-nose capabilities to separate the Fingerprint/Skydrol clusters from interferent. Moreover, each Skydrol/Fingerprint concentration level is detected when GDA-fr is employed.

**Table 4** Total amount of data sampled by PC-Method

Data sampled by PC-Method		
	GDA-fr	SNIFFI
FP-1	3	3
FP-2	4	3
FP-3	3	7
ALL	28	28

*FP* refers to Skydrol contaminated samples at low (1), medium (2) and high (3) concentration level. *ALL* includes not Skydrol contaminated samples: untreated (Reference) plus interferences (TD, DI) samples

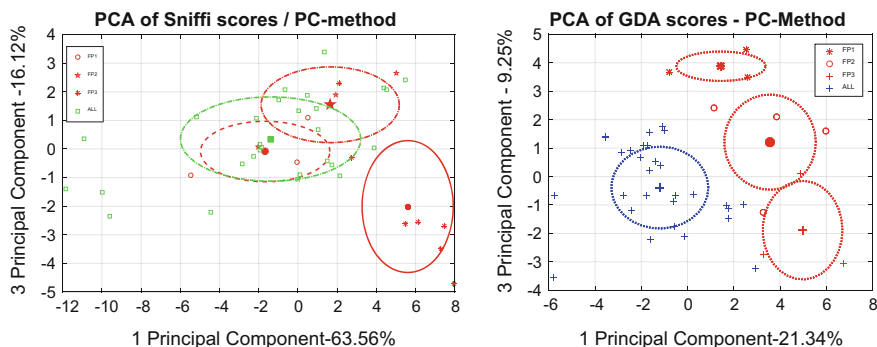


**Fig. 6** Cluster of PCA scores related to Sniffi and GDA-2 response sampled by PC-method

Taking advantage of PC-method capabilities to enhance the surface contamination, an classification rate and the concentration level of Fingerprint/Skydrol contamination will be computed starting from data sampled by means of PC-method.

## 4 Results

This section is devoted to briefly illustrate and compare the first classification and regression results achieved on data sampled by PC-method for both devices. First of all, we explore e-noses capabilities to discriminate Fingerprint/Skydrol (FP) contaminated samples from all other types of contamination. At this aim, reference samples, thermal degraded samples and de-icer contaminated samples are labeled as interferences, constituting a single class named 0-class, while 1-class will contain FP contaminated samples at each contamination level. So, we are dealing with a binary and unbalanced classification problem, because of the highest number of interferent samples respect to FP contaminated ones. The classical machine algorithms provide for both device acceptable correct classification rate. Specifically, Sniffi data measurements are correctly classified, by a linear classifier, as Skydrol contaminated at 73.2% with an false negative rate equals to 31%, as it can be read in the confusion matrix (Fig. 7). The area under the ROC curve (AUC) is set to 0.74 underlying a good tradeoff between TP/FP.

Otherwise, a decision tree classifier provides a correct classification rate for GDA-fr enose equals to 97.4% with a false negative rate set only at 10%, and a AUC near to 1 (Fig. 8).

So, depending on the employed e-nose, different classification results are achieved. Nevertheless, they seem to be perfectly consistent with different separation capabilities highlighted in the previous PCA analysis leading to likewise different estimations in the contamination level. Specifically, regression results are computed taking advantage of a two layers feed forward neural network with ten hidden neurons, trained with Bayesian regularization backpropagation algorithm.

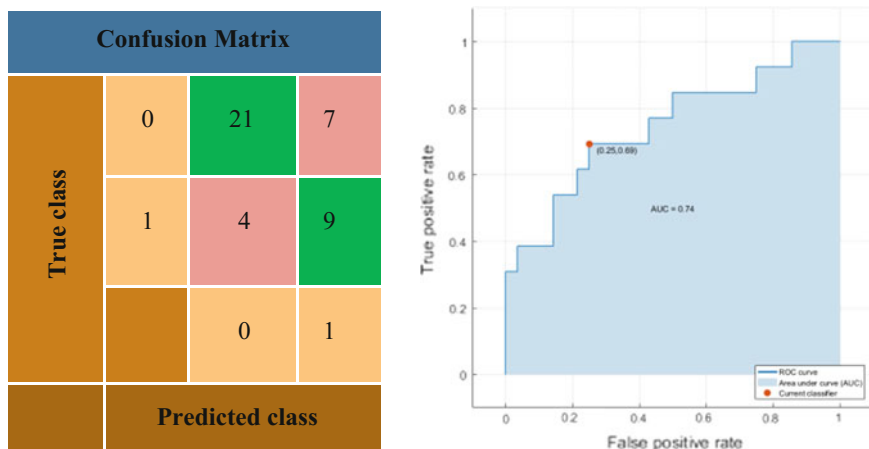


Fig. 7 Confusion matrix and ROC curve for linear discriminant

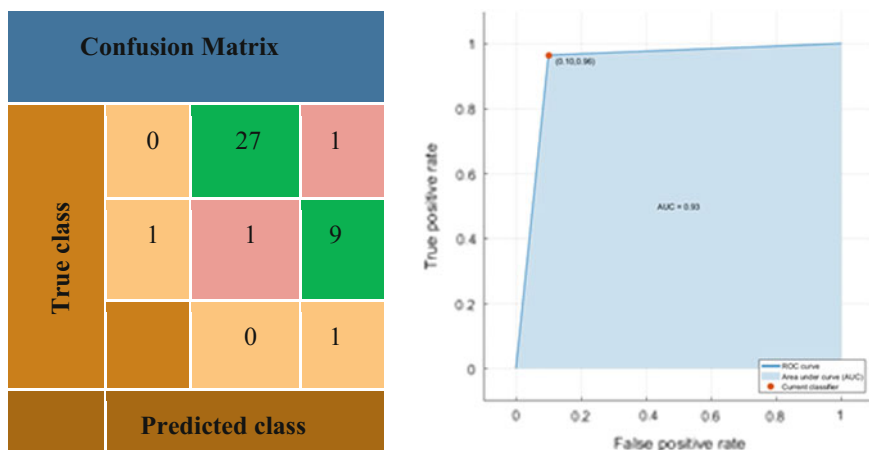
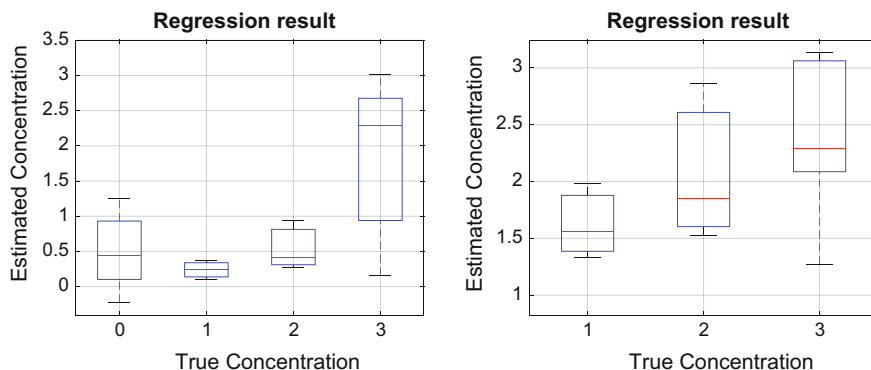


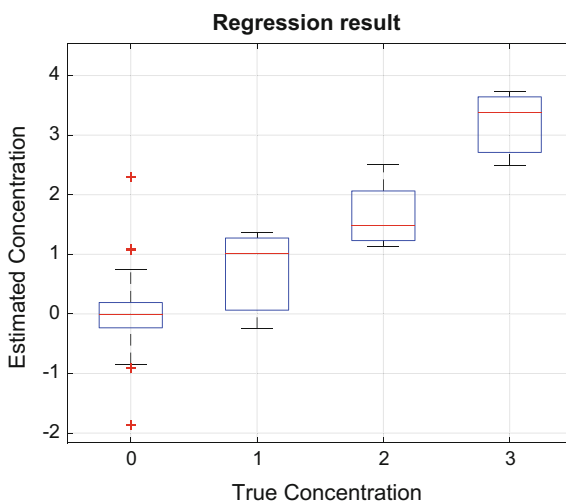
Fig. 8 Confusion matrix and ROC curve related to decision tree classifier

The three different Fingerprint/Skydrol concentration levels are labeled with '1', '2', '3' tag respectively for the low, medium and high contaminated class. Otherwise, label 0 is used to indicate the true concentration level of the interferences class. In Fig. 9 (left), boxplots relating to SNIFFI regression results underline a marked trend to under-estimate all three FP levels when their concentration levels are computed together with 0-level. The mean absolute error is set to 0.72. Otherwise, regression results, after FP detection contamination, show an improvement on the FP-contamination level estimation mainly into the 2nd and 3rd level (Fig. 9-right).



**Fig. 9** Sniffi estimation boxplots of concentration level of interferences class (0) and FP classes (1-2-3) (on the left); on the right boxplots related to concentration levels of three FP contaminated classes

**Fig. 10** GDA-2 estimation boxplots of concentration level of interferences class (0) and the three FP classes (1-2-3)



Different considerations can be done about GDA-2 regression results. As it can be seen in Fig. 10, this e-nose provides a good estimation of the interferences and FP-1 contamination level, being the respective medians exactly equals to the correspondent true concentration value.

Other FP concentrations levels (FP-2; FP-3), instead, are slightly under and over estimated respectively. Anyway, their variability range always includes the correspondent true concentration level. So, regression results confirm the PCA findings about GDA-fr sampled data that yet underlined as the FP-1 cluster and interferences cloud are clearly distinguishable from other FP contaminated samples. The others out estimated FP levels can be again explained in PCA terms: their ellipses being tangent (Fig. 6) gives rise to simple misunderstanding. Finally, the Mean Absolute

Error computed on GDA-fr regression results being equals to 0.37 confirms clearly the best performance of this device with respect to SNIFFI e-nose setting.

## 5 Conclusions

In order to uplift the TRL of NDT technologies for detection of Fingerprint/Skydrol oil contamination at low concentration levels, two different e-noses technologies (SNIFFI, ENEA e-nose and GDA-fr commercial solution) and two sampling method (0- and PC-Method) are explored. PC sampling method enhances contaminants cluster separation of both devices mitigating Sniffi limitations and allowing to detect and estimate Fingerprint/Skydrol oil at least at the highest COMBONDNT concentration level. With the same methodology, the GDA-2 capabilities extends to the quantification of the level of contamination that is actually present on the samples.

**Acknowledgements** This work has received funding from the European Union's Horizon 2020 research and innovation programme under grant agreement No 636494, Project name COMBONDNT.

## References

1. Timmis, A.J., Hodzic, A., Koh, L., et al.: Environmental impact assessment of aviation emission reduction through the implementation of composite materials. *Int. J. Life Cycle Assess.* **20**, 233 (2015)
2. COMBONDNT Project Website, <http://combondt.eu>. Accessed 9 May 2017
3. Markatos, et al.: Effects of manufacturing-induced and in-service related bonding quality reduction on mode-I fracture toughness of composite bonded joints for aeronautical use. *Composites B*, **45**, 556–564 (2013)
4. The ENCOMB Project Final Report Summary—[http://cordis.europa.eu/result/rcn/156281\\_en.html](http://cordis.europa.eu/result/rcn/156281_en.html). Accessed 9 May 2017
5. Salvato, M., et al.: An holistic approach to e-nose response patterns analysis—an application to non-destructive tests. *IEEE Sens. J.* **16**(8), 2617–2626, April 5 (2016). doi:[10.1109/JSEN.2015.2513818](https://doi.org/10.1109/JSEN.2015.2513818)
6. Van den Bergh, J., et al.: Aircraft maintenance operations: state of the art (2013)
7. Foster, S.K., Bisby, L.A.: Fire survivability of externally bonded FRP strengthening systems. *J. Compos. Constr.* **12**(5), 553–561 (2008)